# Knudsen Self- and Fickian Diffusion in Rough Nanoporous Media

Kourosh Malek and Marc-Olivier Coppens[*]

*Physical Chemistry and Molecular Thermodynamics,*

*Delft Chem Tech, Faculty of Applied Sciences, Delft University of Technology*

*Julianalaan 136, 2628 BL Delft, The Netherlands*

The effect of pore surface roughness on Knudsen diffusion in nanoporous media is investigated by dynamic Monte-Carlo simulations and analytical calculations. A conceptual difference is found between the roughness dependence of the macroscopic, transport diffusivity and the microscopic, self-diffusivity, which is reminiscent of diffusion in zeolites, where a similar difference arises due to adsorption effects and intermolecular interactions. Because of the dependence of the self-diffusivity on molecular residence times, self-diffusion may be roughness dependent, while transport diffusion is not. Detailed proofs are given. The differences become significant when the pore surface is rough down to molecular scales, as is the case, *e.g.*, for many common sol-gel materials. Simulations are in good agreement with analytical calculations for several tested rough, fractal pore structures. These results are important for the interpretation of experimental diffusion measurements and for the study of diffusion-reaction processes in nanoporous catalysts with a rough internal surface.

Keywords: Diffusion; nanoporous materials; fractals, self-diffusivity; roughness.

---

[*]Corresponding author: Tel: +31-15-278 4399; Fax: +31-15-278 8668
E-mail: M.O.Coppens@tnw.tudelft.nl

**Contents**

## I. Introduction

The physics of diffusion in disordered media has attracted a lot of attention, due to its significance in major technological areas such as catalysis, electrochemistry and separations [1-5]. One of the main challenges in modelling heterogeneous catalytic processes is the realistic representation of the texture of the porous catalyst [3,5,6]. The most frequently used modelling approach is to consider the catalyst particle as a pseudo-homogeneous system where the diffusion of reactants and products is described by effective diffusion coefficients [7]. Such continuum models may serve as an approximation for some monodisperse catalysts or catalysts with well connected pores [8], but more realistic network models are generally preferred. When continuum models or parallel pore models are used, different effective diffusivities may be obtained by various experimental and operating methods, because the detailed catalyst geometry influences the results [9].

In a heterogeneously catalysed reaction, molecules diffuse through the pore network, collide with the pore walls and react on active sites on these walls. The topology of the pore network and the morphology of the pores affect the molecular movements and the accessibility of the active sites. Hence, the diffusivities of the components and, therefore, the conversion and product distributions of the reactions as well as the rate of catalyst deactivation may depend on the catalyst geometry [10-12]. In recent years, much effort has been devoted to the study of diffusion in disordered networks [3,5]. The effect of network *topology*, and in particular pore interconnectivity, can be accounted for by using methods from statistical physics, such as percolation theory, renormalization group theory and Monte-Carlo simulation [3,13]. Such studies were also performed to study viscous flow in sandstones and other porous rocks, where both topological and morphological effects are known to influence the permeability [13]. Pores are usually represented as straight cylindrical channels in order to considerably simplify the simulation procedures [8-10]. More complicated shapes have been considered to test the effect of the pore shape on diffusion [14]. Others have attempted to represent the complex catalyst morphology by randomly superposing solid spheres [15] or by subtracting spheres and cylinders from a solid matrix [16] with diffusion in the remaining pore space studied by a Monte-Carlo method. The effects of detailed pore shape and surface *morphology* are usually ignored, either because of problems in modelling them realistically [17], or because their influence is assumed to be negligible.

In many applications involving gases in mesoporous materials, which are materials with most pore sizes between 2 and 50 nm, Knudsen diffusion is the predominant transport mechanism. Knudsen diffusion is a result of collisions of gas molecules with the pore walls, rather than intramolecular collisions (Brownian motion), so that the effect of the wall roughness should be investigated [18]. There is experimental evidence for the fractal roughness of the internal surface of many amorphous catalysts over a finite scaling range that includes the size of typical diffusing molecules [19,20]. The irregular catalyst morphology and its influence on diffusion and reaction can therefore be modelled in a realistic way using fractal geometry. Fractal pore models therefore can be used to study the effect of surface roughness on Knudsen diffusion. Smoluchowski already showed in 1910 that pore shape in general has an effect on Knudsen diffusion [21]. An analytical formula was derived for fractal pores by Coppens and Froment [22,23] indeed predicting a considerable effect of surface roughness on the Knudsen diffusivity. However, Santra and Sapoval [24] performed simulations that showed no such effect. Experimental evidence seems contradictory as well [25]. Recently reported experimental results by Geier et al. [26] show that the apparent tortuosity factor in the Knudsen regime may be significantly larger than that in the bulk regime for one and the same porous medium. The observed difference between the tortuosity factors in the bulk and Knudsen regimes may have its origin in the different influence of the geometrical details, *i.c.*, roughness, of the intercrystalline pore surface on diffusion.

To resolve this apparent disagreement, we recently performed dynamic Monte-Carlo simulations of Knudsen diffusion in two- and three-dimensional fractally rough pores [27]. These simulations showed that the origin of the discrepancy might lie in an up to now neglected difference between self- (or tracer) and transport (or collective) diffusivities in rough mesopores, with results for the self-diffusivity that are in agreement with earlier analytical predictions [27-29].

The difference between the parametric dependence of self- and transport diffusivities is well recognized for zeolites, where self- and transport diffusion depend in a different way on molecular concentration, because molecules interact with each other. In the Knudsen regime, however, molecules move independently of each other so that a similar difference, now as a function of roughness, seems less obvious. In this paper, we present detailed analytical models and calculations, supported by dynamic Monte-Carlo simulations, showing that the self-diffusivity has the predicted roughness dependence, while the transport diffusivity is roughness independent, at least when the molecules only interact with the walls

upon collision. Because of the qualitative generality of the derivations, results are independent of the details of the roughness model, and also hold for non-fractal geometrically heterogeneous systems. The fractal pore model, however, enables us to compare analytical results with dynamic Monte-Carlo simulations.

## II. Roughness dependence of Knudsen diffusivity

Gas molecules move through a channel in a porous solid. In the Knudsen diffusion regime, the molecules do not interact with one another, so that they move in straight lines between points on the pore channel surface. Upon collision with the surface, a molecule adsorbs for a brief time. The direction of a molecule again leaving the surface is independent of the direction of incidence and follows Lambert's cosine law, similar to diffuse light scattering. Surface roughness is sometimes quoted as the reason for this cosine distribution law, but it has been shown already more than 70 years ago that it is fundamental in nature and can be extracted from the principle of microscopic reversibility and the second law of thermodynamics [22,30]. The time of physical adsorption on the surface is neglected with respect to the time of flight, although its effect may be easily included [29]. Statistical methods, *e.g.*, finite-passage time methods, can be used to find the roughness dependence of the Knudsen diffusivity, accounting for the molecular accessibility distribution over the pore surface. Using such a model, diffusion can be simulated in a general porous medium with a fractal internal surface. However, since we focus on surface morphological effects only, and in order to avoid the topological effect of pore networks, we will consider a single pore. The results remain valid for pore networks as well, if morphology and topology are uncorrelated [22,23,31]. Note also that percolation effects only come about in situations where the connectivity is low, the molecules large, the pore size distribution very wide, or blocking occurs [3,8].

## A. Knudsen self-diffusion

Self-diffusivity is a measure of the translational mobility of individual molecules. Under conditions of thermodynamic equilibrium, a molecule is tagged and its trajectory followed over a long time. If the motion is diffusive, and in a medium without long-range correlations, the squared displacement of the molecule from its original position will eventually grow linearly with time (Einstein's

equation). To reduce statistical errors in simulations, the self-diffusivity, $D_s$, of a species $i$ is defined

from ensemble averaging Einstein's equation over a large enough number of molecules, $N$ :

$$D_s = (\frac{1}{6N})\sum_{k=1}^{N}\lim_{t\to\infty}\frac{1}{t}\left\langle \left|\vec{r}_k(t)-\vec{r}_k(0)\right|^2 \right\rangle \qquad (1),$$

where $\vec{r}_k(t)$ is the position of the $k$-th molecule of species $i$ at time $t$. Only one species is considered,

since species diffuse independently of each other in the Knudsen diffusion regime, so the index $i$ will

generally be dropped in the notations. The self-diffusivity is easily shown to be equivalent to the *tracer*

diffusivity [32,33]. Its observation necessitates some labeling of the molecules involved. In usual

experimental measurements of the self-diffusivity, a tracer technique is used, where a fraction of the

diffusing species is distinguished from the remaining molecules, *e.g.*, by the use of isotopes, without

affecting their mobility.

Using a finite passage time calculation, a practical and simple expression for the roughness

dependence of Knudsen self-diffusion in a porous medium with a fractal internal surface has been

derived. Only the main results will be summarized here, as a general derivation of this analytical formula

both in 2D and 3D can be found in [22,28].

A general pore with a fractal surface can be mentally constructed by a fractal perturbation on top

of a pore with a smooth surface. In 2D, the surface reduces to two fractal lines. Along the pore, there are

a large number of fjords with a hyperbolic (power law) size distribution within the fractal

range, $\left[\delta_{\min}^s, \delta_{\max}^s\right]$ (Fig.1). As a result of the finite inner cutoff $\delta_{\min}^s$, there is a finite probability,

$(\delta_{\min}^s / \delta_{\max}^s)^{2-D_c}$ , for a molecule not to enter any 3D fjord, but just hit a segment of unperturbed pore

wall. $D_c$ is the fractal dimension of the cross-section of the fractal surface with the smooth unperturbed

surface. In order to estimate geometric diffusivity changes with roughness, the effects of all surface

specifications should be considered, yet these can be collected into two parameters, namely: the fractal

dimension of the surface, $D_{ads}$ , and the return probability, $p_0$ , which is the probability for a molecule to

leave a fjord, once it is in it [22]. The above model can account for the non-uniform accessibility, leading

to the following expression for the Knudsen self-diffusivity [22,28]:

$$\frac{D_s}{D_s^0} = \frac{1}{1 + \alpha[1 - (\delta')^\beta]}$$ (2),

in which $D_s^0$ is the Knudsen self-diffusivity in the unperturbed medium with the same overall topology

and pore volume as the real porous medium, but a Euclidean smooth surface, and $\delta' = \delta / \delta_{max}^S$ is the

normalized effective diameter of a molecule of size $\delta$. In 2D and 3D, the parameters $\alpha$ and $\beta$ can be

analytically calculated from $D_{ads}$ and $p_0$ [22]. For smaller molecules or a larger outer cutoff (small $\delta$)

the reduction in Knudsen self-diffusivity is stronger, because of the restrictions imposed on the molecular

movement.

Since the above procedure is based on a perturbation of smooth pore walls, the effect of a

possible increase in pore volume resulting from the fractal perturbation in a self-similar fractal pore, as

compared to the unperturbed pore space, must be accounted for. Assume a 3D Koch pore with average

diameter $\overline{d}$ and a regular polygonal cross-section with $Q$ edges, *i.e.*, for a square cross-section $Q = 4$, and

for an octagonal cross-section $Q = 8$. Also assume that $M_C$ is the number of cubes located on top of any of

the $N_S$ surface segments of the generator in any iteration step, $n$, and that the edge of a cube of the

generator is reduced by a factor of $1/\lambda$ after each generation. The general equation for the increase in

enclosed pore volume, $V_n$, upon constructing a fractal 3D Koch pore from a smooth pore, with enclosed

volume $V_0$, is [28]:

$$V_n = V_0 \left\{ 1 + M_C \times \frac{Q}{(\lambda^3 - N_S)} \times \left(\frac{\delta_{max}^s}{\overline{d}}\right)^2 \left[ 1 - \left(\frac{N_S}{\lambda^3}\right)^n \right] \right\}$$ (3).

In calculations for 3D pores with a deterministic fractal surface, Knudsen diffusivity should be corrected

for pore volume changes upon perturbing the pore space, by using this equation. For the statistically self-

similar pore walls considered in the Monte-Carlo simulations in section III, the average volume or area

change is zero by construction.


**B. Knudsen Fickian (transport) diffusion**

Fickian diffusivity $D_t$ is defined as proportionality constant between the macroscopic flux $J$ and

the negative of the concentration gradient $\vec{\nabla} C$:

$$J = -D_t \vec{\nabla} C \qquad\qquad\qquad\qquad\qquad\qquad (4).$$

Most practical applications of molecular transport in nanoporous materials occur under nonequilibrium conditions, in which a macroscopic concentration or chemical potential gradient is present. The transport or collective diffusion coefficient $D_t$ accounts for the collective motion of particles under the influence of a concentration gradient, as opposed to the self- or tracer diffusion coefficient $D_s$, which quantifies the individual microscopic motion of the molecules. There is a whole class of macroscopic experiments available that probe the transport diffusivity, such as uptake rate measurements [34], permeation rate measurements [35], and frequency response analyses [36]. Just very recently, two microscopic techniques have become available that measure intracrystalline transport diffusion [37,38]. Up to now, only few simulation techniques have been developed for diffusion under conditions where the system is not in thermodynamical equilibrium [39]. The nonequilibrium simulation techniques all try to mimic an experimental technique: either a relaxation experiment (where an initial chemical potential gradient is allowed to relax), or a steady state experiment (where the gradient is kept constant by an external force field). Both methods probe the same property, *i.e.*, the transport diffusion coefficient. This is in contrast to the self-diffusion coefficient, which is typically evaluated at thermodynamic equilibrium, either in experiments as the (equivalent) tracer diffusion coefficient in a PFG-NMR measurement or in simulations by calculating the mean-square displacement of tracer particles in a system without gradients. To our knowledge, the roughness dependence of transport diffusion in the Knudsen regime has not been theoretically investigated. Very recent Grand Canonical Molecular Dynamics Simulations (GCMDS) of diffusion in a single pore and simulations of transport in a packed-bed column with mesoporous particles show that transport diffusion is hardly influenced by pore structure and pore roughness [40,41]. In this section, we derive an explanation of this experimental finding, which corroborates our earlier theoretical predictions [27]. We also refer to the analysis of the simulation method that is used further on in this paper for evaluating the transport diffusivity.

Let us first look at the schematic pore diagram in Fig. 2. In this illustration, any type of perturbation, whether it comes from geometrical irregularity (*e.g.*, a pore with rough fractal walls in mesoporous materials) or chemical inhomogeneity (*e.g.*, adsorption sites in crystalline microporous zeolites) is represented as a *trapping* zone. During diffusion, a molecule may enter a trap (collide with the walls of a

fjord or adsorb on a lattice site), stay there for a while, and then leave the trap. In the following discussion, we describe the effect of these geometrical or chemical traps on the transport diffusivity. This representation refers to a system in the presence of trapping barriers (since the framework is inert, there is no energetic barrier). Molecules enter the pore from a reservoir (concentration $C_0$) on the left (A) and leave the pore either on the same side (A) or on the other side (C), where there is a vacuum (zero concentration). There is a so-called *entrance effect* for transport diffusion, meaning that not all molecules entering the left side (A) of the pore should be considered, but only those crossing a certain cross-section B inside the pore, to allow them to equilibrate. When molecules leave the pore again through the entrance A, before ever reaching B, they are out of consideration, also in the simulations discussed in Section III. We now argue and will prove that the probability for a molecule to leave the right side (C) once it has crossed B is independent of roughness.

Let us refer to the situation described earlier for a smooth (unperturbed) and perturbed pore wall. In both cases transport diffusivity is defined on the basis of the fraction of molecules leaving the pore through the opposite side, say, in the positive $z$ direction. This fraction is the transmission coefficient $f_t$. There are many results, starting with Clausing in the 1930, which show that the transmission probability, even in smooth pores, is a non-linear function of pore length [30]. Changes in chemical potential in directions perpendicular to the pore axis are zero, because there can be no net transport in such directions (second law of thermodynamics). In the steady state, this is the basis for the fact that transport diffusivity is the same for pores with a smooth and a rough surface. For a better understanding of the problem, we look at a fjord or "trap" and what can happen there during diffusion of molecules in the Knudsen diffusion regime inside the pore. First consider a smooth, unperturbed pore. Vectors related to the individual steps along the trajectory of a molecule can be projected on a Cartesian coordinate $(z)$, where the $z$-axis coincides with the pore axis:

$$\vec{l}_{z,j} = proj_{\vec{z}}(\vec{l}_j) \tag{5},$$

in which $\vec{l}_j$ is the step vector between collision points $j-1$ and $j$. Assume that after $M$ collisions with the wall, the molecule leaves the pore of length $L - L_{eq}$ ( $L_{eq}$ is equal to the AB equilibrium distance or

entrance zone in Fig.2). Then, for $N$ molecules entering the pore during a time $\tau$, the transmission factor can be expressed as:

$$f_t = \frac{\sum_{n=1}^{N}\left|\sum_{j=1}^{M(n)} proj_{\vec{z}}(\vec{l}_j)\right|}{N.(L-L_{eq})} = \frac{\sum_{n=1}^{N}\left|proj_{\vec{z}}\sum_{j=1}^{M(n)}(\vec{l}_j)\right|}{N.(L-L_{eq})} \qquad (6),$$

since the innermost sum has a length of either 0 or $L-L_{eq}$, and the vectors are collinear.  Now, consider a pore with a rough surface. Diffusion in that pore is similar to diffusion in a smooth pore with traps, in which a molecule jumps along the unperturbed surface instead of colliding with the walls within a circle of diameter $u$, corresponding to the inlet diameter of a fjord or indentations (Fig. 3). If $\vec{\varepsilon}_j$ is the imaginary jumping vector along the unperturbed surface, the transmission probability is given by:

$$f_t = \frac{\sum_{n=1}^{N}\left|proj_{\vec{z}}\sum_{j=1}^{M(n)}(\vec{l}_j+\vec{\varepsilon}_j)\right|}{N.(L-L_{eq})} \qquad (7).$$

For a large number of molecules with collisions in a long enough pore, Eq. (7) converges to Eq. (6), *i.e.*,

$\sum_{n=1}^{N}\left|proj_{\vec{z}}\sum_{j=1}^{M(n)}\vec{\varepsilon}_j\right| \rightarrow 0$, because of the principle of microscopic reversibility, *i.e.*, for each step there is one statistically equiprobable step in the opposite direction. This holds for any situation where the inter-step correlations in the trajectory are finite, as is the case for a long rough pore or a lattice representative of a pure Si zeolite. The pore has to be long enough for the sums to converge: consider the diffusion of molecules in a long cylindrical channel with traps (Fig. 2). When the molecules enter the pore via side A, they can get trapped and stay in each trap for a period of time. Molecules can leave the pore again via the inlet A, or leave it through the other side C. However, there should be enough traps along the trajectory for the trajectory steps to be uncorrelated and the transmission probability to become independent of trapping. This means that only molecules that pass a cross-section B should be considered to avoid entrance effects that can affect transport diffusivity values. Past the equilibration length AB, the number of molecules that cross B and exit through C does not depend on the number and distribution of traps anymore. This is important in the calculation of transport diffusivity values from Monte-Carlo simulations.

The above expressions also show that the transmission probability (Eq. 7) and, therefore, the transport diffusivity, are merely a function of the way collision angles are distributed and possible correlations of the molecules with the walls or "traps". Because for both smooth and rough pores the collision angle follows a cosine distribution, there is no effect of roughness on transport diffusivity under steady state conditions.

### III. Dynamic Monte-Carlo simulations

### A. Methodology

Model fractal pores are generated in a similar way to our previous work [27-29,42]. A typical three-dimensional pore segment is shown in Fig.4. The pore surface consists of statistically self-similar Koch surfaces that are recursively generated using an iterative construction algorithm, which repeatedly replaces square tiles by a reduced copy of the generator [43]. Applying this generator in random directions generates a random fractal pore, while a deterministic fractal pore is formed if the generator rule is always applied in the same direction. The variables are pore width, length, and number of generations $n$ (or outer/inner cut-off). The irregularity or roughness factor $\xi$ of a three-dimensional pore at any generation is characterized by the ratio of the pore surface area of the rough pore to the pore surface area of an unperturbed smooth pore with the same average cross-sectional area. For example, for the 3D pore in Fig.4, $\xi = (13/9)^n$ where $n$ is the iteration number or order of the applied fractal generator [28].

Different fractal generators produce pore structures with different values of the fractal dimension and return probability $p_0$ (Fig. 5a). Pores constructed from these generators have a different lacunarity [43]. Lacunarity is a counterpart to the fractal dimension and describes the texture of a fractal. It is related to the size distribution of the holes. Roughly speaking, if a fractal has large gaps or holes, it has high lacunarity; on the other hand, if a fractal is almost translationally invariant, it has low lacunarity. Different fractals can be constructed that have the same dimension but look widely different because they have different lacunarity. In order to understand the effect of the pore shape and make quantitative comparisons with experiments, the pore cross-section could also be changed, *e.g.*, simulations could be performed on pores with a polygonal cross-section that is closer to a circular cross-section (Fig. 5b).

The simulation procedure of particle trajectories is an extension of the one used in our former studies [27-29]. We consider an orthonormal Cartesian coordinate system positioned in such a way that the z-axis is parallel to the direction of the pore axis, while the x-axis is parallel to one of the sides of the cross-section. A test molecule is assigned a random initial position, either at the inlet (transport diffusion) or in the middle of the pore (self-diffusion). This molecule moves for a distance $l_1$ in a random direction until it hits the system boundary. If the impact position lies on the pore surface, it is saved as the first collision point. The molecule is assumed to undergo a diffuse reflection at this point, as explained elsewhere [18,30]. We take the same unit of time in all our simulations, which is the time needed to cross a length equivalent to one pore diameter. Assuming an independent velocity distribution, for sufficiently long trajectories consisting of subsequent moves $l_j$, the time spent is directly proportional to the distance.

In this context, it is interesting to mention that Smoluchowski showed the velocity distribution to be different from the classical Maxwell distribution for Knudsen diffusion [21]. If the collision point lies on the inlet or outlet boundary sides of the pore volume, the molecule leaves the pore volume or may re-enter it through the opposite end. In the latter case, the boundaries are virtual, since periodic boundary conditions in the z-direction are applied. This allows saving computer memory for the representation of long and complex pores.

The molecules in our computations are represented by point mass particles, so that the results are approximate to order $\delta \sim \delta_{\max}^s / 3^n$; molecules of size $> \delta$ cannot see features smaller than $\sim \delta$. A hard sphere potential for the collision with the walls is assumed. Application of molecular dynamics [44,45] and grand canonical ensemble Monte-Carlo simulations [46] would allow for a more accurate analysis of the collision and diffusion dynamics. Here, a purely mesoscopic geometrical approach is presented, which allows us to focus on effects induced exclusively by the pore geometry.

The self-diffusivity, $D_s$, is obtained from Einstein's relation, Eq.1, after calculating the end-to-end square displacement and the total trajectory length in an infinitely extended pore following a large number of collisions, and ensemble averaging over a large number of molecules. On the other hand, imposing a concentration gradient over a pore of finite length $L$, using the same simulation program for the collisions as when simulating self-diffusion, yields the transport diffusivity. Since the molecules move independently in the Knudsen regime, transport diffusion can be investigated by releasing molecules "one

by one" from one end of the pore and studying their motion until they leave the pore. The possible presence of other components (binary or multi-component mixtures) is unimportant, since in the Knudsen regime different species do not interact, by definition, so that our results are relevant to mixtures as well. Results are averaged over a sufficient number of molecules, so that the results become time independent: we are studying the transport diffusion process in the steady state. When a molecule exits the real pore inlet or outlet, it does not re-enter through the other side, but periodic boundary conditions may be applied to parts of the pore. A crucial point in these transport simulations is the consideration of the aforementioned (section II-B) entrance effects near the inlet, *i.e.*, it is necessary to remove molecules that cannot enter deeply into a pore (not more than $L_{eq} \cong 20\delta_{max}^{s}$). Removing this effect is important, as it eliminates the artificiality of correlations of the motion with the specific shape of the inlet region, by allowing the molecules to equilibrate after crossing a few segments. Transport diffusion is therefore considered over the pore stretching out from the equilibration length, *e.g.*, from point B on until the other pore end C, and with respect to the imposed concentration gradient over this same piece, $(C_B - 0)/(L - L_{eq})$ (see Fig.2). In other words, the fraction of molecules that leave the pore through the far end, C, is calculated with respect to those that have crossed the equilibration length at B. The transport diffusivity, $D_t$, is evaluated using Eq. (4), which can be expressed as a function of the transmission probability, $f_t$, *i.e.*, the fraction of equilibrated molecules that leave the pore on the other side:

$$D_t = J \frac{(L - L_{eq})}{C_B} = f_t \frac{C_B \bar{u}}{4} \times \frac{(L - L_{eq})}{C_B} = f_t \frac{\bar{u}(L - L_{eq})}{4} \tag{8}.$$

In comparing smooth and rough pores, it suffices to compare the respective transmission probabilities $f_t$, as the other parameters are the same; the average molecular velocity is independent of roughness and given by the kinetic theory of gases, $\bar{u} = \sqrt{8RT/\pi M}$. Eq. (8) shows that the entire roughness dependence of the transport diffusivity is included in $f_t$. Knudsen [47] showed that for a very long cylindrical smooth pore with diameter $d$, $f_t = \frac{4d}{3(L - L_{eq})}$, so that $D_t = \frac{d\bar{u}}{3}$, while Clausing [30] derived equations for pores of arbitrary finite lengths. In our simulations, we therefore aim to verify our

analytical prediction that the transmission probability of long pores ($L \gg L_{eq}$) is roughness independent.

## B. Discussion of the results

A typical example of part of a trajectory in a 2D fractal pore is shown in Fig. 6a. In contrast to the case of a smooth pore, the relative number of short distances covered by a molecule between two successive collisions increases enormously when the degree of irregularity is increased. Our earlier studies [27,28] showed that the corresponding distribution of the individual trajectory segments is a power law within the (normalized) fractal scaling range [$3^{-n}$,1], so that the trajectories are *Lévy flights* with an outer cutoff on the order of the largest fjord size (Fig. 6b). An important property of systematic Lévy processes is the fact that they are subordinated to ordinary Brownian motion: the corresponding probability density function (PDF) of the steps $x$, normalized with respect to the inner cutoff $\delta_{min}^{s}$ ($l_j = x \cdot \delta_{min}^{s}$), can be represented in the form:

$$p(x) = \int_0^\infty \frac{1}{\sqrt{2\pi\tau}} \exp\left(-\frac{x^2}{2\tau}\right) p(\tau) d\tau \tag{9}$$

$$= \int_0^\infty \frac{1}{\sqrt{2\pi\tau}} \exp\left(-\frac{x^2}{2\tau}\right) \frac{\alpha}{\tau^{1+\alpha/2}\sqrt{2\pi}} \exp\left(-\frac{\alpha^2}{2\tau}\right) d\tau$$

$$= \frac{2^{(1-\alpha)/2}}{(x^2+\alpha^2)^{(3-\alpha)/2}} \cdot \frac{\alpha}{\pi} \Gamma\left(\frac{3}{2}-\frac{\alpha}{2}\right)$$

where $\alpha$ is the Lévy distribution index and the variable $\tau$ is called the operational time of the process [48]. For $\alpha = 1$, this yields the Cauchy distribution. The interpretation of the above equation is that Lévy flights can be considered as stemming from a highly irregular sampling of trajectories generated by simple diffusion (ordinary random walk). Here, the diffusion trajectory (a random walk in a discrete case) is parameterised by the operational time $\tau$ (say, the number of steps of the random walk), which itself is a random function of the physical time. The random process $\tau$(t) is a process with positive increments, and the distribution of $\tau$(t) is given by a Lévy-distribution, having a power law tail, $p(\tau) \propto \tau^{-1-\alpha/2}$. Deviations can occur for very long paths, which are influenced by the shape of the pore and the detailed shape of the generator, as a result of both inner and outer cutoff effects. This is to be contrasted with the

case of the smooth pore. For a two-dimensional smooth pore, $l_j = \overline{d} / \cos(\theta_j)$ and as $p(l_j)dl_j = 2\sin\theta_j \times \cos\theta_j d\theta_j$, one can write:

$$p(l_j) = \frac{2\overline{d}^2}{l_j^3} \qquad\qquad (10).$$

The existence of a Lévy distribution for paths much smaller than the pore width is a specific consequence of the pore irregularity. These results clearly show that for increasingly rough fractal pores, the average of the path length between successive collisions changes from the order of the pore diameter for a smooth pore to the order of the inner cutoff, $\delta_{min}^s$, for a very rough, highly irregular pore [22,27,42].

The effect of pore surface roughness on self- and transport diffusivities is presented as a function of roughness in Fig.7a. For a 3D pore with $\overline{d} = \delta_{max}^s$, there clearly is a large effect of roughness on self-diffusion: the self-diffusivity decreases significantly as the roughness factor $\xi$ increases. On the other hand, the transport diffusivity does not vary with $\xi$ and is therefore independent on roughness in the steady state. These results confirm our analytical predictions and can be explained by considering the conceptual differences between these two kinds of diffusivities. Since the residence time distribution does not affect the transmission probability, transport diffusion is independent on the residence time of individual molecules, so that only the concentration gradient over the pore and the average pore cross-section are important. Figure 7b shows the normalized transmission probability $f_t / f_t^0$ versus diffusion time (where $f_t^0$ is the steady state transmission probability through a smooth pore with the same cross-sectional area as the rough pore). As before, time is normalized with respect to the time needed to cross a length equivalent to one pore diameter. Transmission probability increases with time until it converges after a sufficiently long time. This time is longer for a rough than for a smooth pore. Obviously, the transport diffusivity may only be estimated at steady state. When the diffusion time is not an issue, whether a molecule stays for a long or a short time in a pore does not have any effect on the outlet through which it leaves the pore. Convergence is slower for a rough pore, as a result of the same confinement effects that reduce the self-diffusivity, but the transmission probability in the steady state is roughness independent. In a long enough pore and under the influence of a moderate concentration gradient, the transport diffusivity is therefore not a function of wall surface irregularity either. The latter

is different for self-diffusion, which is an *inherently* direct function of the individual molecular trajectories, the total trajectory length or residence time. Trajectory lengths increase with increasing surface irregularity, and depend on molecular size and shape [21,23,24]. Roughness only has an effect on self-diffusion if it leads to trapping in the axial direction. In order to verify this, we also carried out simulations of diffusion in 3D structures with a 2D fractal cross-section perpendicular to the pore axis, but straight in the axial direction (Fig. 8). This *anisotropic* wall roughness does indeed not affect axial diffusion, as the equal self- and transport diffusion values corresponding to the different fractal generations of the cross-section in Fig.8 demonstrate. These values were corrected for the volume increase after each generation. Fig.8 shows that there is no significant difference between self- and transport diffusion when there is no roughness in the direction of diffusion, *i.e.*, the *z*-axis. The latter is again in agreement with the analytical approach to the roughness independence of transport diffusion in section II, since the transmission probability through the pore only depends on the projection of all the individual collision vectors on the *z*-axis, which is the same for a smooth pore. The MC results can be compared to the analytical solutions for self- and transport diffusion in a random 3D fractal pore on the basis of Eqs. 2 and 7. In the case of self-diffusion, $p_0$ can be calculated from the ratio of the area (corresponding to the length in 2D) of a fjord's opening to the area (length) of its (unperturbed) walls. For the Koch pore models considered earlier, $p_0 = 1/5$ for 3D simulations. Lines in Fig.7a show the analytical calculations. The agreement between these analytical results and the MC simulations is excellent.

As discussed earlier, constancy of the transport diffusivity with varying surface roughness is caused from the independence of the transport fluxes on the residence time of individual molecules. An increase in residence time for a given incoming flux and a constant transmission probability should imply that the molecular concentration in the pore space increases with roughness. Particular attention is necessary here not to confuse an equilibrium with a non-equilibrium situation. The residence time of molecules increases when the surface is rougher. This first produces an increase in molecular concentration inside the pore in a transient situation where the molecules are abruptly started being injected, at clock time zero, from one pore end (*i.e.*, the boundary condition at entrance A is a Heaviside function with step height $C_0$). The concentration is more localized when the surface is rougher, especially near the pore inlet, which leads to the aforementioned entrance effect. Therefore, the

concentration increase compensates for the time-delay that is caused by surface roughness. To analyse and visualize this, we have calculated, at various clock times $t$, the concentration (or molecular density) profile inside rough and smooth pores that connect reservoirs of concentrations $C_0$ (left) and $0$ (right). Fig.9a shows the density profile for a rough pore (second generation, $n$=2) at different clock times. The steady state at $t = t_{\text{inf}}$ was verified. Near the pore inlet, a maximum appears because of the equilibrating entrance effect. Many molecules do not penetrate deeply into the pore, but bounce back into the reservoir on the left, which is kept at a constant concentration $C_0$. This effect is especially pronounced for rough pores, where it leads to a concentration increase in the entrance zone. Such a zone does not appear in a smooth pore (Fig.9b). A density decay in the pore starts after the equilibrium distance. At long enough times, the density profile converges to a curve, which, for rough pores, peaks in the entrance zones, and then drops linearly to a low value near the outlet. For a smooth pore the drop is linear throughout the pore from entrance to outlet (Fig. 9b). The crossing of the entrance zone is harder for a rough pore than for a smooth one, after which the transmission properties are the same. This behaviour is very reminiscent of adsorption and transport diffusion in microporous solids such as zeolites, a similarity that will be discussed in the next section.

The pore diameter has an important effect on the magnitude of the roughness dependence of self-diffusion. In fact, the relevant dimensionless parameter is the ratio of pore diameter to outer cutoff of the surface irregularity, $\bar{d} / \delta_{\text{max}}^s$. When a molecule diffuses through a pore with a high $\bar{d} / \delta_{\text{max}}^s$ value, even with very rough walls in absolute terms, the pore walls act as if they were smooth, so that there is no significant difference with a truly smooth wall, because path segments on the order of $\bar{d}$ dominate diffusion. The effects of $\bar{d} / \delta_{\text{max}}^s$ on the self-diffusivity are presented in Fig.10a. The effect of roughness on self-diffusivity is less pronounced in pores for which the largest surface indentations are considerably smaller than the pore diameter, *i.e.*, $\bar{d} / \delta_{\text{max}}^s$ is large [28]. However, there is a significant roughness dependence for self-diffusion in nanopores with a roughness up to the size of the pores themselves ($\delta_{\text{max}}^s \sim \bar{d}$), a typical situation in sol-gel synthesized disordered materials [20].

In solids with not too narrow pores, combinations of the appropriate transport laws appear to predict the overall transport behaviour very well [49]. We focused on Knudsen diffusion because there

should be no significant effect of the roughness morphology on molecular diffusion, since diffusion in this regime is dominated by intermolecular collisions and therefore only depends on total cross-section void space and not so much on pore wall effects. For Knudsen flow, while the cylindrical pore formula derivation is presented in many places [18,50,51], the effect of a non-circular cross-section on the transport rate is often ignored; nevertheless, the deviations are often small, as it has been shown that the Knudsen equation for flow through circular pores may be used for most porous materials with a non-circular pore cross-section [21,52]. In order to better understand the effect of pore cross-section, pores with cross-sections of different polygonal shapes were constructed. An example was shown in Fig. 5b for the first generation of the fractal generator. Simulations of Knudsen diffusion show similar results to those in pores with a square cross-section, Fig. 10b. The values of the diffusivities are a bit higher in the octagonal pores (the effect of surface roughness is slightly less pronounced), because of the smaller inner cutoff $\delta_{min}^s$ accessible to the diffusing molecules.

In section III-A we introduced fractal generators to construct pores of different lacunarity (different $p_0$). Fig. 11 presents simulation results of self-diffusion in such pores, and compares these to analytical results predicted by Eq. 2 (lines). Increasing $p_0$, the self-diffusivity increases, since a molecule on average stays for a shorter time in each fjord. By increasing the fractal dimension of the pore, the diffusivity goes down, as the surface is rougher. These results again confirm our analytical predictions.


## IV. Comparison with diffusion in zeolites; diffusion in mesopores vs. micropores

The results can also be qualitatively compared to what is known for diffusion in crystalline, microporous zeolites (aluminosilicates). The diffusion mechanisms in zeolites and rough mesoporous materials are different, so the comparison is qualitative at most. In zeolites, molecules are of almost the same size as the pores they are diffusing through, so that diffusion typically consists of activated hops between adsorption sites. The diffusion of a single adsorbed species in zeolites can again be characterized by either the self- or the transport diffusivity [32,33]. The self-diffusivity at a given concentration, $D_s(C)$, measures the displacement of a tagged molecule as it diffuses at equilibrium inside a crystal of a zeolite where the total adsorbate concentration is $C$ (Eq.1). Macroscopic diffusion of a single adsorbed species in zeolites can be characterized by using the transport diffusivity (Eq.4).

Recognizing that the chemical potential is a more appropriate driving force for diffusion than concentration, the transport diffusivity is rewritten as:

$$D_t(C) = D_0(C)\left(\frac{\partial \ln f}{\partial \ln C}\right)$$ 

(11).

Here, $f$ is the fugacity of the bulk phase that is in equilibrium with the adsorbed phase when the latter has concentration $C$, and $D_0(C)$ is called the corrected diffusivity, which is related to the self-diffusivity but is not necessarily identical to it, especially for multi-component mixtures. The term involving the logarithmic derivative of the fugacity is referred to as the thermodynamic correction factor. Note again that each of the three diffusivities defined above, self-, transport and corrected diffusivity, may have other commonly used names. The self-diffusivity is also known as the tracer diffusivity [33]. The transport diffusivity is also referred to as the Fickian diffusivity [53], the chemical diffusivity [54], or the collective diffusivity [55]. Finally, the corrected diffusivity is also known as the jump diffusivity [56]. Tracer and collective diffusion are essentially different, and this difference only disappears when there are no correlations present in the system. This is well known for zeolites, where it is a result of correlations induced by intermolecular interactions. All diffusivities coincide in the limit of very low concentrations, where different molecules do not hinder one another.

Although the actual dependence on molecular loading or concentration depends on the chemical details of the molecule-zeolite system, simple lattice models predict that transport diffusion in a pure Si zeolite (Al/Si=0) is independent of molecular loading, while self-diffusivity decreases with loading [57,58]. For a better understanding of the similarities between what happens in a rough mesoporous material and in a zeolite, consider a one-dimensional line with equivalent sites on which molecules are hopping. Assume a single molecule hopping along this line. If the adsorption is strong, the self-diffusivity decreases, as the motion is slower (molecule randomly hops from site to site). This is like trapping in a fjord in a rough mesopore. The transmission probability, however, is clearly independent of the adsorption coefficient (or trapping strength). In this case, only the time after which the molecule leaves the line is changed, not its overall motion. In short, trapping (from adsorption or roughness) leads to a decrease in self-diffusivity, but not in transport diffusivity, when the imposed gradient is expressed in terms of concentrations of the adsorbed species (equal to species in the pore). Perhaps the name "transport diffusivity" is a misnomer as only the self-diffusivity characterises the truly diffusive behaviour, but the

name has stuck, especially as a way to interpret transport data from a membrane, or as a proportionality factor in Fick's law.

It is interesting to consider how the ideas emerging from the discussion above may apply to several aspects of molecular transport in nanoporous materials. For the diffusion of molecules in mesoporous materials such as MCM-41, we expect that the open nature of the pores in these materials will offer a favourable environment for the transfer of momentum between adsorbates [59]. Reyes et al. [60] provided a phenomenological description of diffusion in porous solids. In their description, molecules within a zeolite crystal only move in an adsorbed state so that surface diffusion is the only mode of transport (Eq. 11), unlike the case of mesoporous materials in which the possibility of a dual transport mechanism involving gas and surface diffusions is well documented. The steric effects that cause a rapid decrease in self-diffusivities as a function of loading in micropores [61,62], also exist in rough amorphous mesoporous materials, as we have just demonstrated. It is suggested that whenever trapping occurs in microporous or mesoporous materials, self-diffusivities will rapidly decrease with pore loading, but transport (collective) diffusivities will be a much weaker function of pore loading.


## V. Conclusion

In summary, both our simulations and analytical calculations show that surface roughness can affect self-diffusivity of gas molecules in the Knudsen regime. This is particularly so when the pores are (fractally) rough and perturbed on the same scale as the local pore diameter. The latter is the case for many sol-gel based catalysts and supports. On the other hand, our simulations as well as our mathematical analysis of the molecular trajectories in smooth and rough pores showed the independence of transport diffusivity on surface roughness. This results from the fact that the projection of the molecular trajectory pathway in a pore with a rough surface is equivalent to that in a pore with a smooth surface when the molecule performs surface jumps around regions on the order of the diameter of the fjord inlet size. These jumps quickly decorrelate, hence the transmission probability is roughness independent. Calculations were performed for pore structures with different cross-sections, fractal dimensions and lacunarity. All simulation results are in good agreement with analytical calculations. The self-diffusivity is the more fundamental diffusivity, expressing how the position of a molecule changes with time as a result of its random motions, influenced by its environment. The total trajectory length is influenced by this

environment; a rougher surface corresponds to more molecular traps along the surface and leads to a decrease in self-diffusivity, whereas transport diffusion or transmission probability are unaffected by the presence of these traps.

**VI. Acknowledgements**

**References**

[1] P.M. Adler, *Porous Media: Geometry and Transport* (Butterworth-Heinemann, Stoneham MA, 1992).

[2] *The CRC Handbook of Solid State Electrochemistry*, edited by P.J. Gellings and H.J.M. Bouwmeester (CRC press, 1997).

[3] M. Sahimi, G.R. Gavalas and T.T. Tsotsis, Chem. Engng Sci. **45**, 1443 (1990).

[4] R. Aris, *The Mathematical Theory of Diffusion and Reaction in Permeable Catalysts*, vol.1. Clarendon Press, Oxford, 1975.

[5] F.J. Keil, Catal. Today **53,** 245(1999).

[6] M.P. Hollewand and L.F. Gladden, Chem. Engng Sci. **47**, 2757(1992).

[7] A. Burghardt, J. Rogut and J. Gotkowska, Chem. Engng Sci. **43**, 2463(1988).

[8] L. Zhang and N.A. Seaton, Chem. Engng Sci. **49**, 41(1994).

[9] S. Arbabi and M. Sahimi, Chem. Engng Sci. **46**, 1749(1991).

[10] G.F. Froment and K.B. Bischoff, *Chemical Reactor Analysis and Design* (2nd ed., Wiley, New York, 1990).

[11] C.K. Lee and S.L. Lee, Surf. Sci. **339**, 171(1995).

[12] C. McGreavy, J.S. Andrade, K. Rajagopal, Chem. Engng Sci. **47**, 2751(1992).

[13] M. Sahimi, *Rev. Mod. Phys*. **65**, 1393(1993).

[14] Y. Nakano, S. Iwamoto, I. Yoshinaga, and J.W. Evans, Chem. Engng Sci. **42**, 1577(1987).

[15] M.H. Abbasi, J.W. Evans, and I.S. Abramson, A.I.C.H.E. J. **29,** 617(1983).

[16] V.N. Burganos and S.V. Sotirchos, Chem. Engng Sci. **44**, 2451(1989).

[17] *Physical and Chemical Aspects of Adsorption and Catalysts*, edited by B.G. Linsen (Academic Press, London, 1970).

[18] D.H. Davis, J. Appl. Phys. **31**, 1169(1960).

[19] D. Avnir, D. Farin and P. Pfeifer, Nature **308**, 261(1984).

[20] M.-O. Coppens, Coll. Surf. A **187-188**, 257(2001).

[21] M. von Smoluchowski, Ann. Phys. **4F**, 1559(1910).

[22] M.-O. Coppens and G.F. Froment, Fractals **3**, 807(1995).

[23] M.-O. Coppens and G.F. Froment, Chem. Engng Sci. **50**, 1013(1995).

[24] S.B. Santra, and B. Sapoval, Phys. Rev. E **57**, 6888(1998).

[25] D.G. Huizenga and D.M. Smith, A.I.C.H.E. J. **32**, 1(1986).

[26] O. Geier, S. Vasenkov and J. Kärger, J. Chem. Phys. **117**, 1935(2002).

[27] K. Malek and M.-O. Coppens, Phys. Rev. Lett. **87,** 125505(2001).

[28] K. Malek and M.-O. Coppens, Coll. Surf. A **206**, 335(2002).

[29] M.-O. Coppens, K. Malek, Chem. Engng Sci. in press.

[30] P. Clausing, Ann. Phys. **5F**, 567(1930).

[31] M.-O. Coppens and G.F. Froment, Chem. Engng Sci. **50**, 1027(1995).

[32] J. Kärger and D.M. Ruthven, *Diffusion in Zeolites and other Microporous Solids* (Wiley, New York, 1992).

[33] D.N. Theodorou, R.Q. Snurr ans A.T. Bell, *Comprehensive Supramolecular Chemistry; Molecular Dynamics and Diffusion in Microporous Materials* (Pergamon, Berlin, 1996).

[34] D. M. Ruthven, R.I. Derrah, and K. F. Loughlin, Can. J. Chem. **51**, 3514(1973).

[35] D.T. Hayhurst and A.R. Paravar, Zeolites **8**, 27(1988).

[36] N. Van-Den-Begin, L.V.C. Rees, J. Caro, and M. Bülow, Zeolites **9**, 287(1989).

[37] U. Schemmert, J. Kärger, and J. Weitkamp, Microporous Mater **32**, 101 (1999).

[38] H. Jobic, J. Kärger, and M. Bee, Phys. Rev. Lett. **82**, 4260 (1999).

[39] F. Müller-Plathe, S.C. Rogers, and W.F. van Gunsteren, J. Chem. Phys. **98**, 9895(1993).

[40] T. Düren, S. Jakobtorweithen, F.J. Keil and N.A. Seaton, Phys. Chem. Chem. Phys. **5**, 369(2003).

[41] M.R. Schure, R.S. Maier, D.M. Kroll and H.T. Davis, Anal. Chem. **74**, 6006 (2002).

[42] M.-O. Coppens, *Fractals in Engineering*, edited by J. Lévy -Vehel, E. Lutton and C. Tricot (2nd edition , Springer, Berlin, 1997), p. 336.

[43] B.B. Mandelbrot, *The Fractal Geometry of Nature* (Freeman, San Francisco, 1982).

[44] J.M.D MacElroy and S.-H. Suh, J. Chem. Phys. **106**, 8595(1997).

[45] L.A. Pozhar, Phys. Rev. E **61,** 1432 (2000).

[46] L.F. Xu, M. Sahimi and T.T. Tsotsis, Phys. Rev. E **62**, 6942(2000).

[47] M. Knudsen, Ann. Phys. **4F**, 75 (1909).

[48] J. Klafter, M.F. Shlesinger, and G. Zumofen, Phys. Today **49**, 33(1996).

[49] J. Kärger and D. Freude, Chem. Eng. Technol. **25**, 769(2002).

[50] S.K. Bhatia and J.S. Gupta, Rev. Chem. Engng **8**, 177(1992).

[51] J.W. Evans, M.H. Abbasi and A. Sarin, J. Chem. Phys. **72**, 2967(1980).

[52] V.N. Burganos and S.V. Sotirchos, Chem. Eng. Sci. **44**, 2451(1989).

[53] S.M. Auerbach, Int. Rev. Phys. Chem. **19**, 155(2000).

[54] C. Uebing and R. Gomer, J. Chem. Phys. **100**, 7759(1994).

[55] D.S. Sholl, Ind. Eng. Chem. Res. **39**, 3747(2000).

[56] C.H. Mak, H.C. Andersen and S.M. George, J. Chem. Phys. **88,** 4052(1988).

[57] M.-O. Coppens, A.T. Bell and A.K. Chakraborty, Chem. Engng Sci. **53**, 2053(1998).

[58] D.S. Sholl and K.A. Fichthorn, Phys. Rev. Lett. **79,** 3569 (1997).

[59] E.J. Maginn, A.T. Bell and D.N. Theodorou, J. Phys. Chem. **97,** 4173(1993).

[60] S.C. Reyes, J.H. Sinfelt and G.J. DeMartin, J. Phys. Chem. B **104**, 5750(2000).

[61] A.I. Skoulidas and D.S. Sholl, J. Phys. Chem. **106**, 5058(2002).

[62] F.J. Keil, R. Krishna and M.-O. Coppens, Rev. Chem. Engng **16**, 71(2000).

**Figure captions**

**Fig. 1.** Schematic representation of an unperturbed (a) and a perturbed (b) surface.

**Fig.2.** Schematic illustration of the cross-section of a pore with perturbed walls; any type of perturbation is represented as a trapping zone.

**Fig.3.** Comparison of the real motion in the vicinity of the rough pore walls with the equivalent effective motion projected on to the unperturbed pore surface.

**Fig.4.** Segment of a 3D pore with square cross-section and a random, second-generation Koch surface for which $\xi = (13/9)^2$.

**Fig.5.** (a) Generators of Koch surfaces with different return probability, $p_0$. $D_c$ is the fractal dimension of the cross-section of the fractal surface with the smooth, non-perturbed surface, which is a Sierpiński carpet in this case [28]. New pores with a high value of $D_f$ can be constructed using variations on such generators. (b) 3D fractal pore generator with octagonal cross-section.

**Fig.6.** (a) Typical example of part of a trajectory in 2D, as calculated by computer simulations. (b) Histogram of the path length $l_i$ between two successive collisions, for pores with a $\xi = (5/3)^3$ degree of irregularity (roughness). The line shows the outer cutoff of the fractal-scaling region. Dashed line shows the power law behaviour as $N_{col}(l) \sim l^{-\alpha}$ and $\alpha = 0.55$.

**Fig.7.** (a) Self- and transport diffusivity as a function of the roughness $\xi$. The lines show analytical results using a first-passage time approach, while the points show dynamic Monte-Carlo results. (b) The normalized transmission probability $f_t / f_t^0$ versus diffusion time; $f_t^0$ is the transmission probability through a smooth pore in the steady state ($t \rightarrow \infty$). One unit is the time to traverse a distance $\delta_{min}^s$ equal to the inner cutoff.

**Fig.8.** Simulation results of diffusion in a 3D pore with a 2D fractal cross-section but straight along the pore axis (anisotropically rough pores).

**Fig.9.** Molecular density profile along a pore. (a) Density profile for a rough pore [ $\xi = (13/9)^2$ ] after different clock times ( $t_{inf}$ is a long time, when steady state is reached). (b) Comparison of the density profiles in a smooth and in a rough pore.

**Fig.10.** Effect of (a) the ratio $\overline{d} / \delta_{max}^{s}$ and (b) the shape of the pore cross-section on the roughness dependence of the self-diffusivity.

**Fig.11.** Simulation results for diffusion in pores of different lacunarity. (a) $D_c \cong 1.89$; (b) $p_0 = 1/5$. The lines show analytical results using Eq. 3.

Figure 1

(a)



(b)
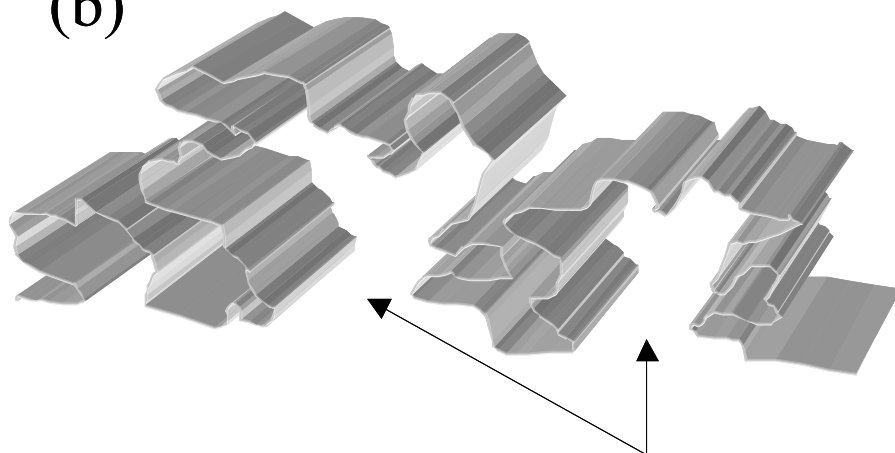
Fjords

Figure 2
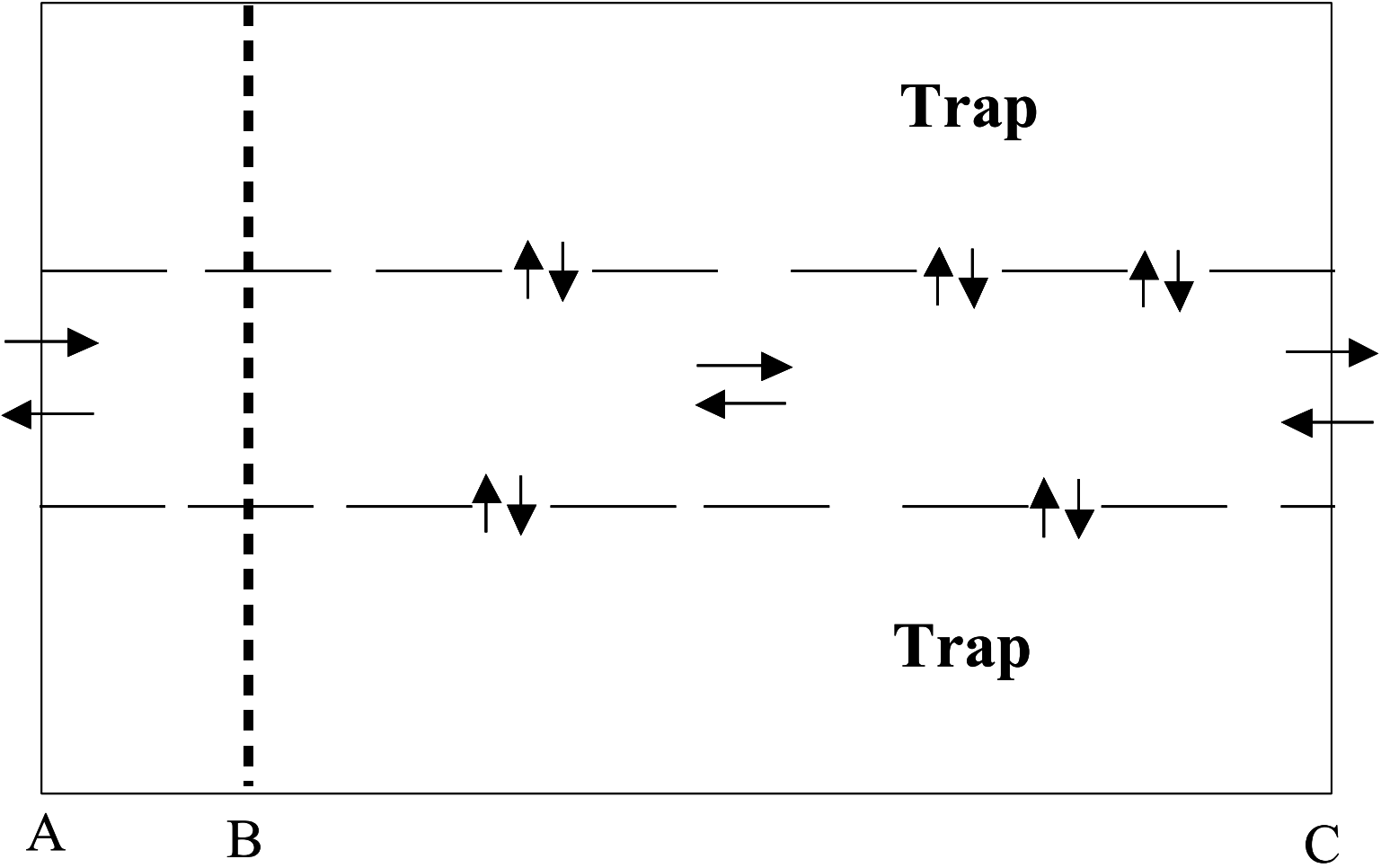
Figure 3
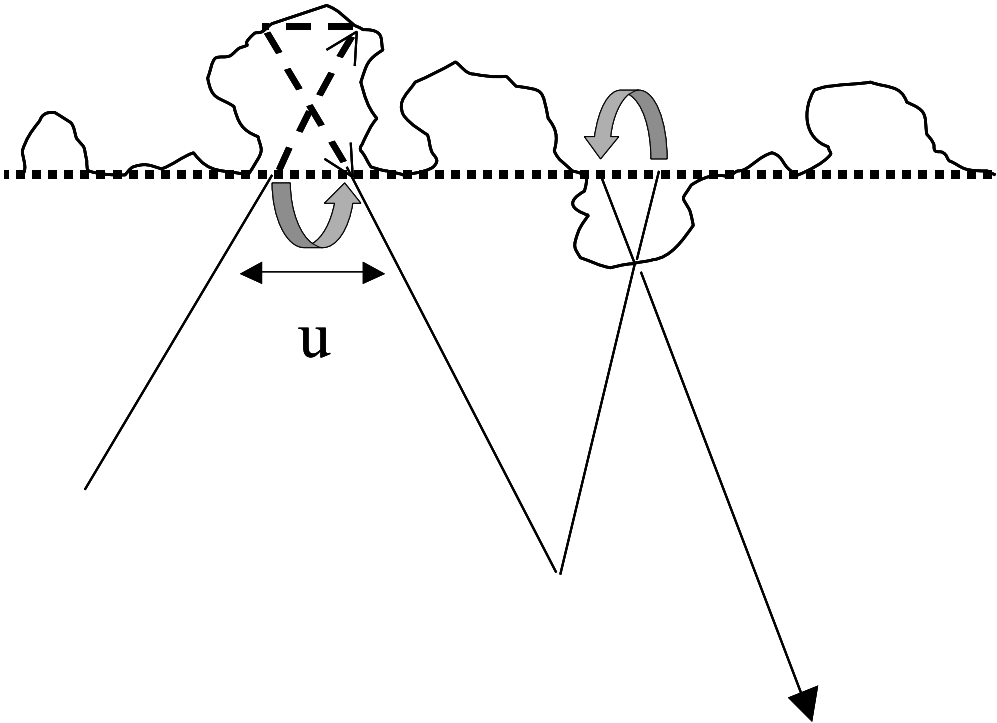


Equivalent jump on the unperturbed smooth surface

Collision pathways in a fjord

Figure 4



**Inlet**
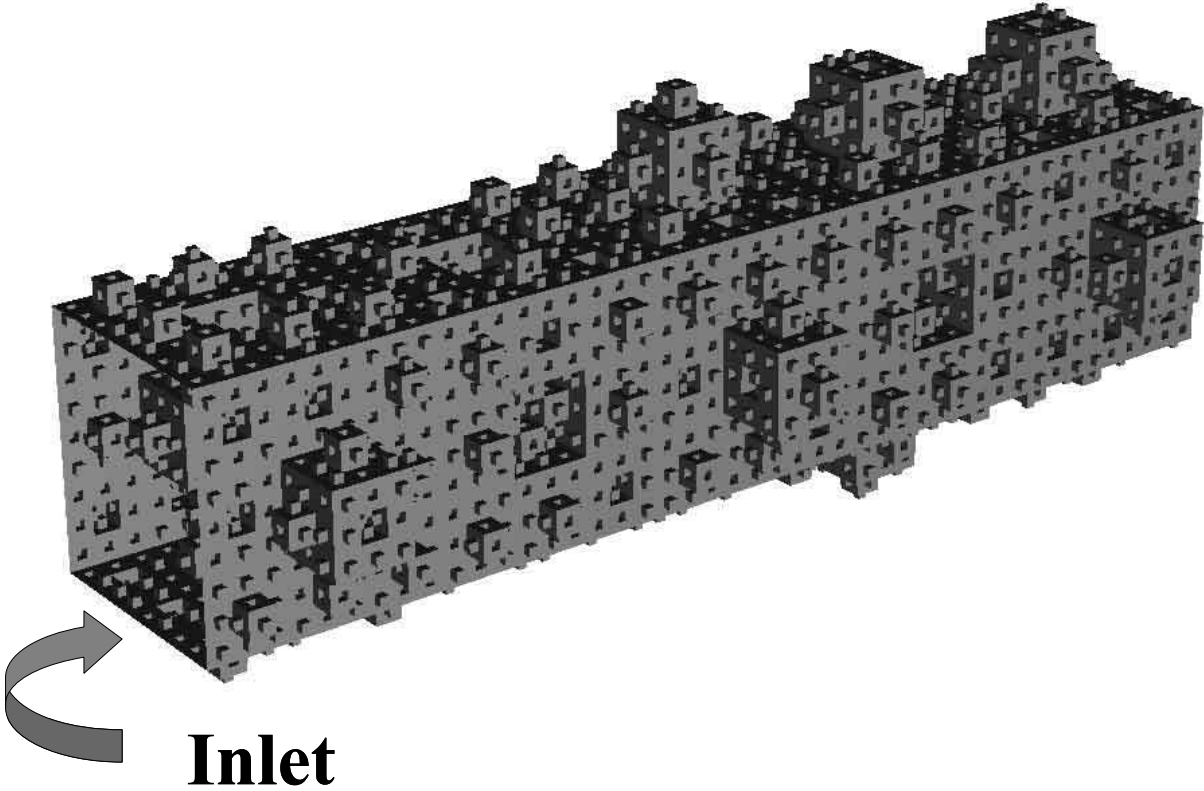
Figure 5a

$D_c$=1.97, $p_0$=1/5

a/5

2a/5

$D_c$=1.97, $p_0$=1/9

a
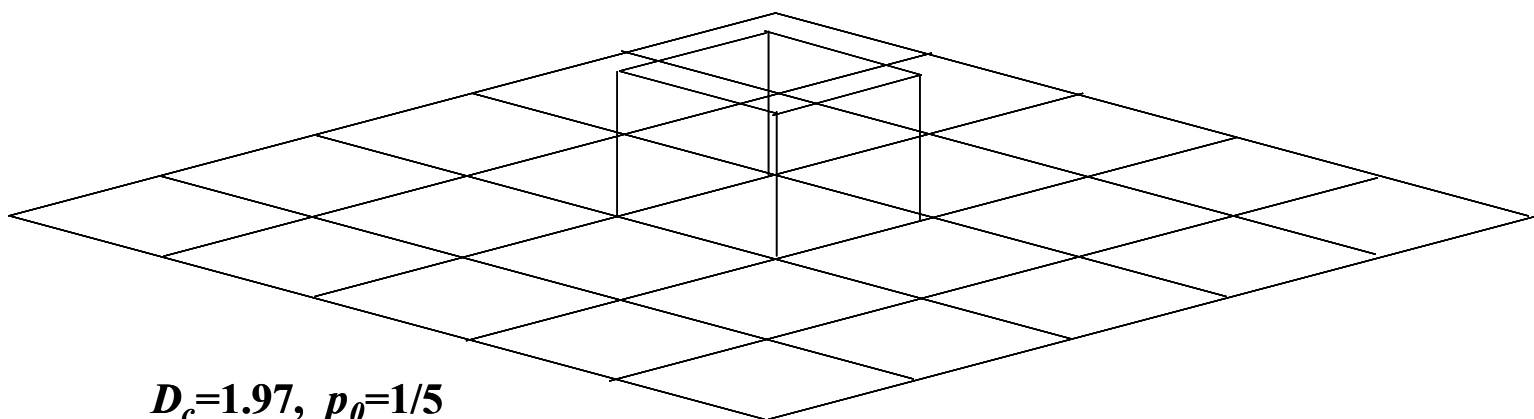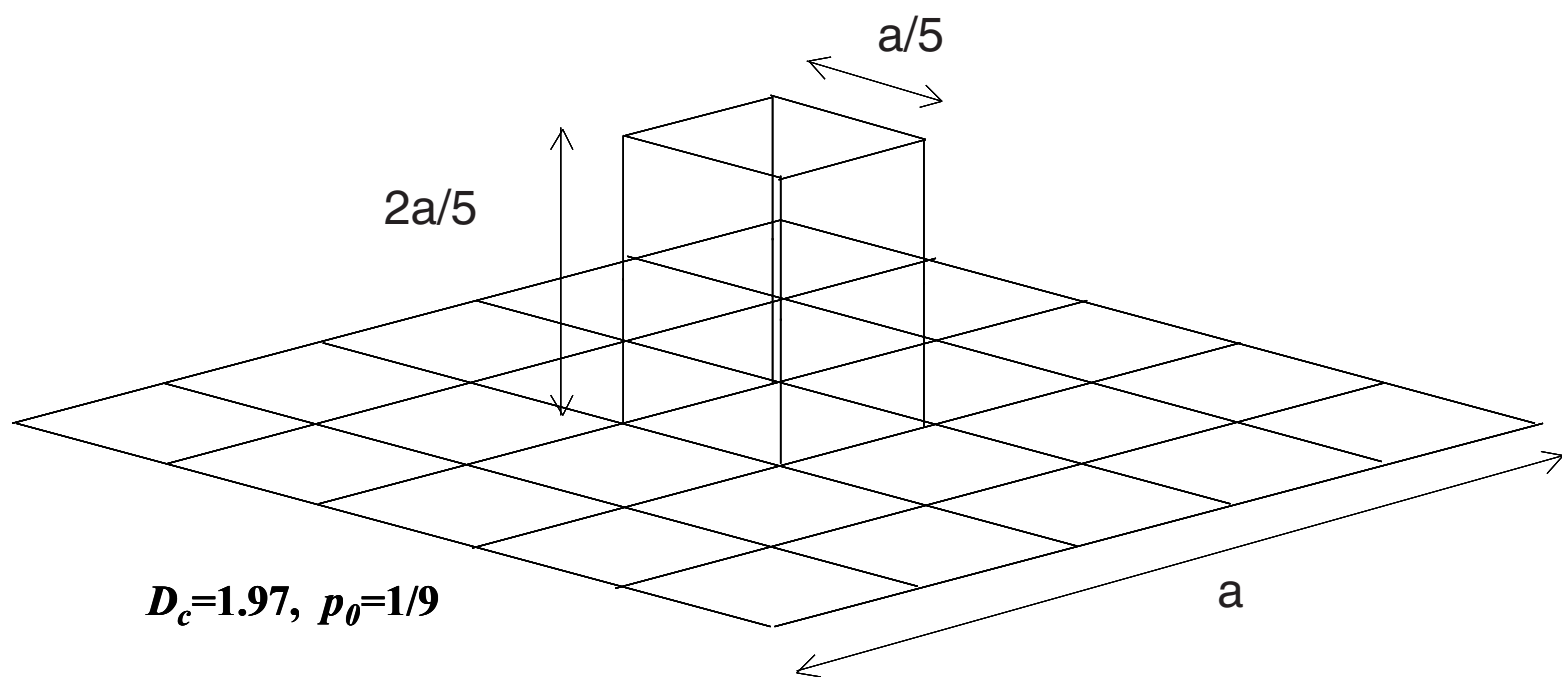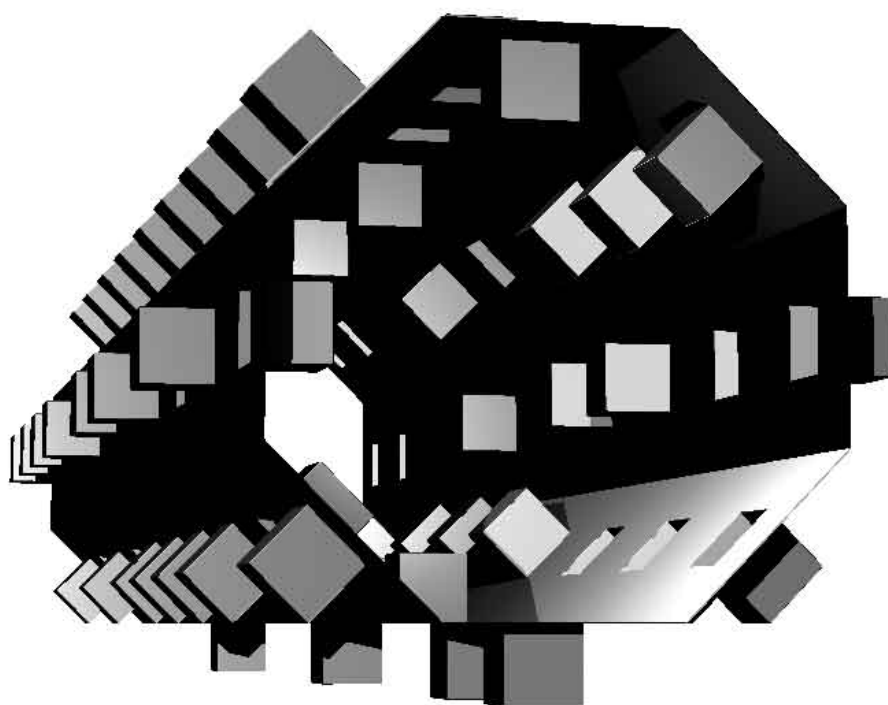
Figure 5b

Figure 6a
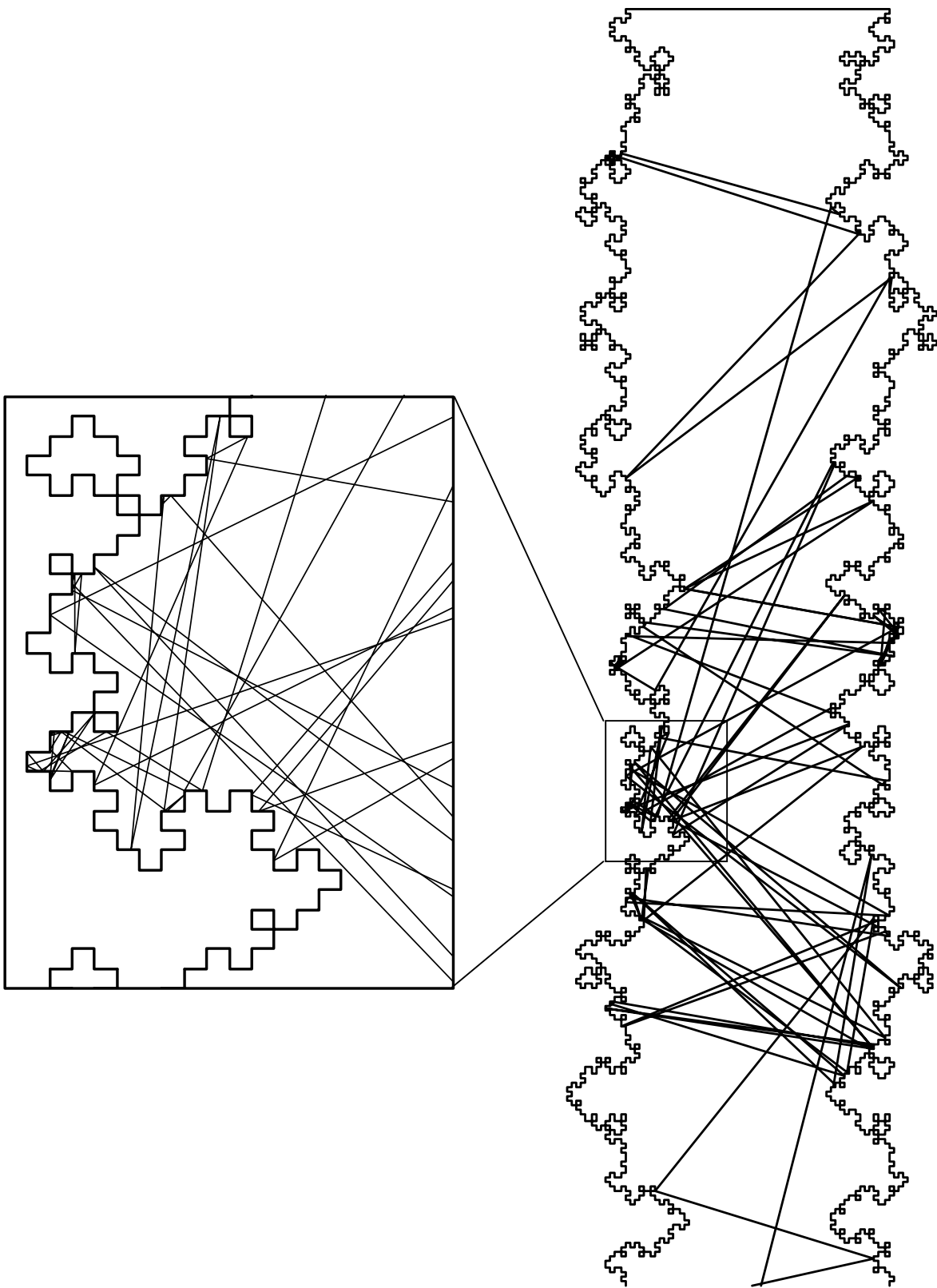
Figure 6b
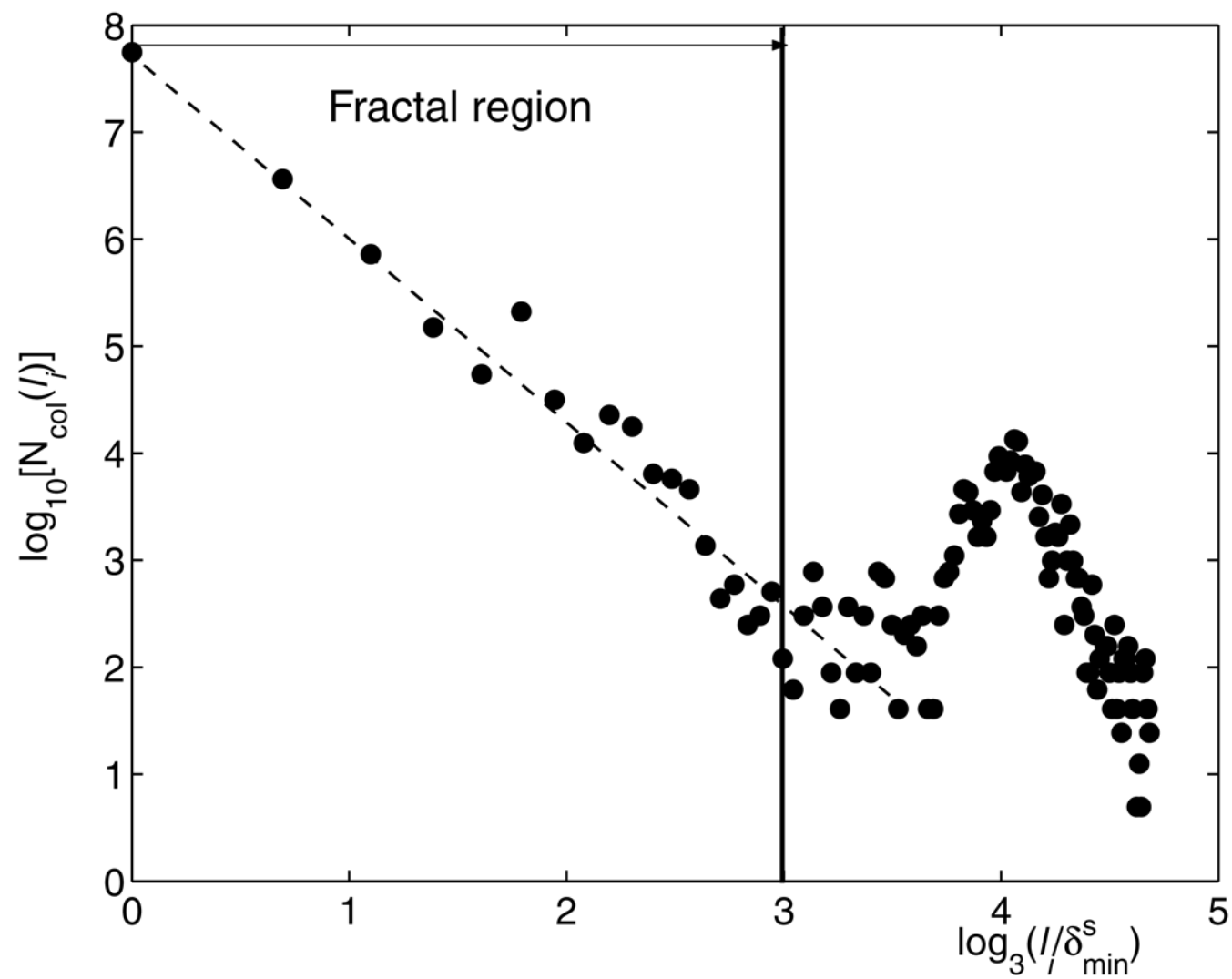
Figure 7a
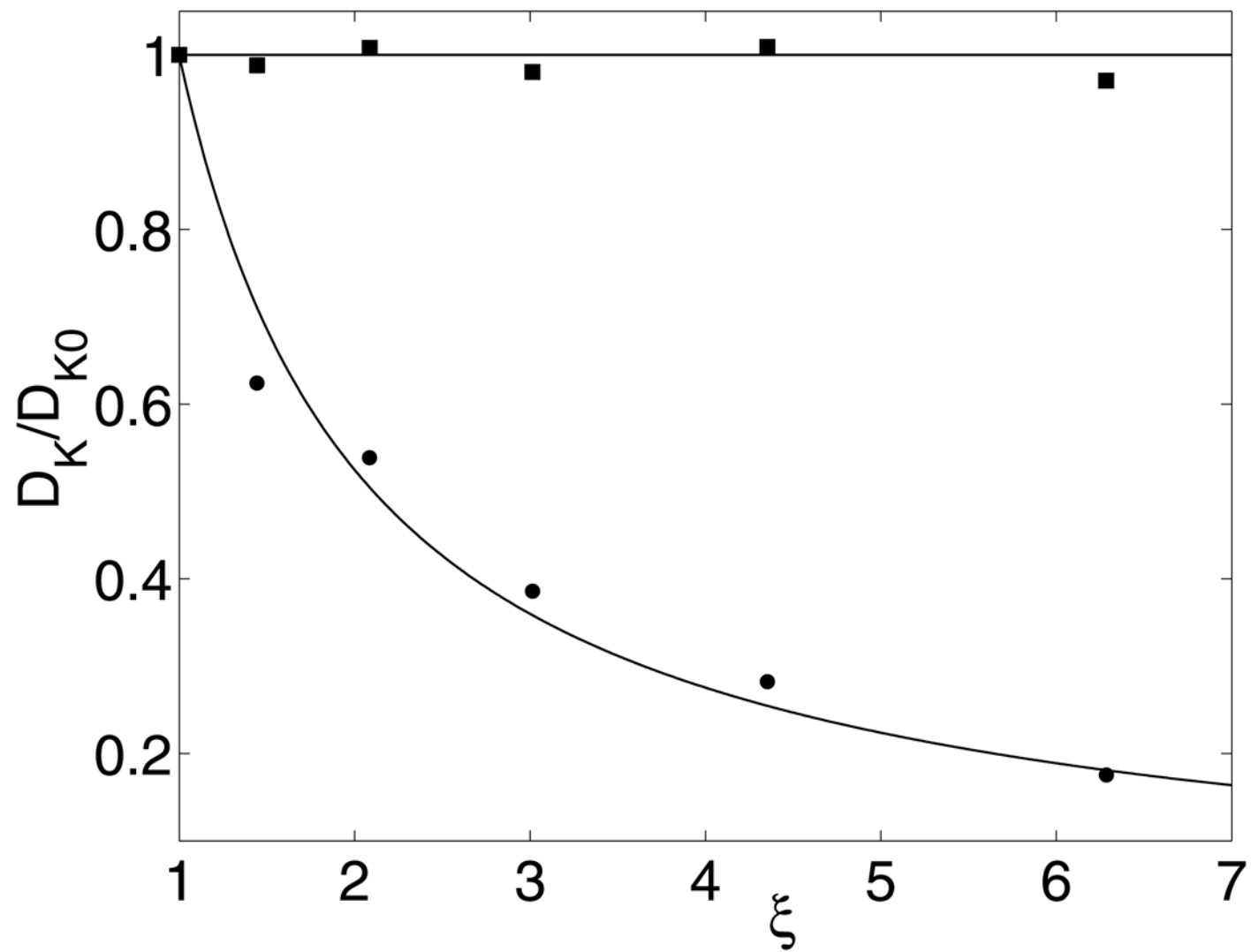
Figure 7b
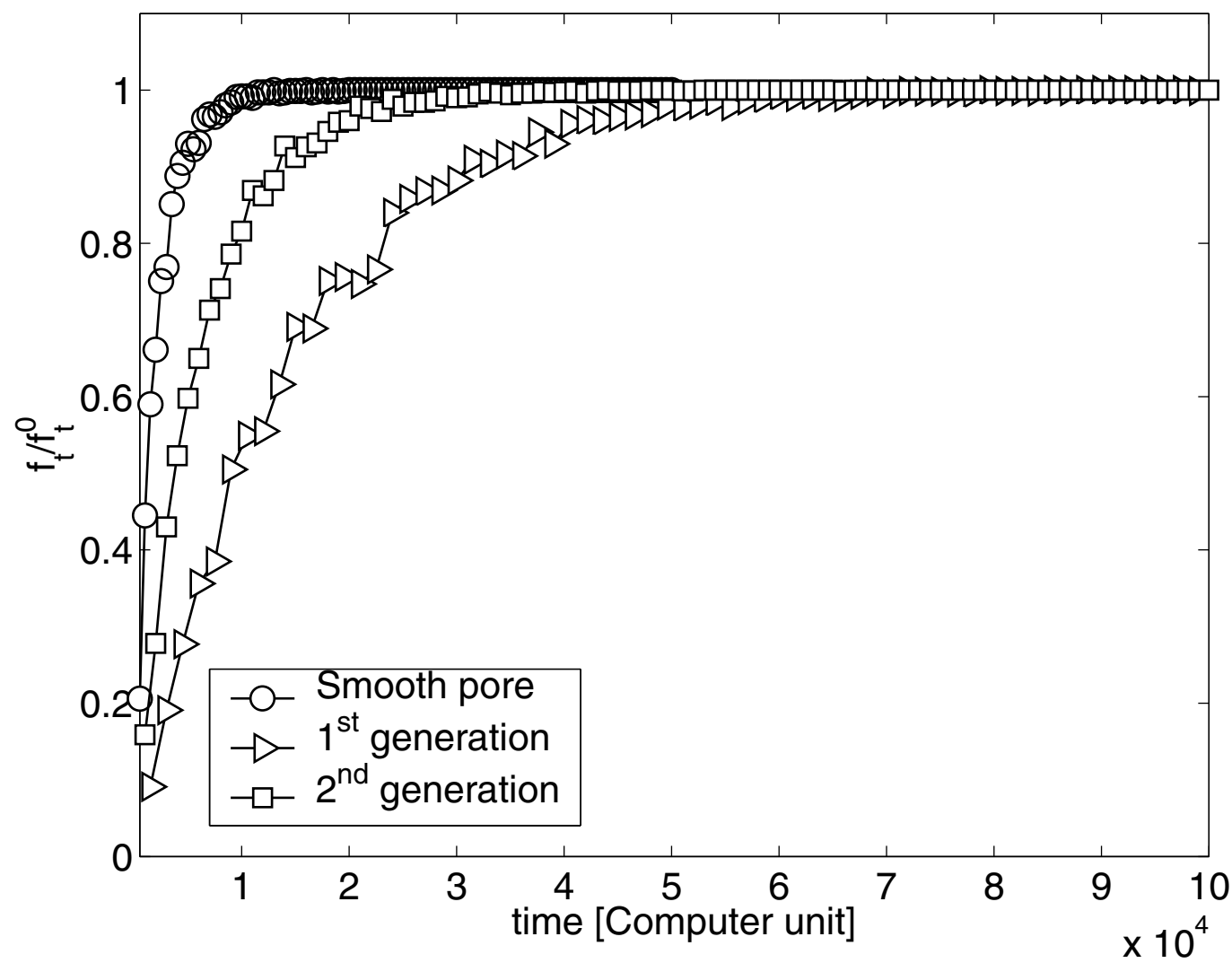
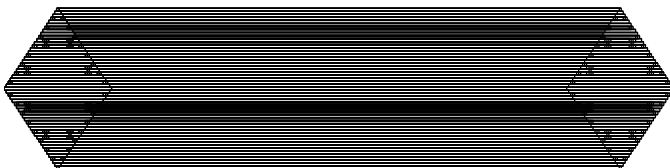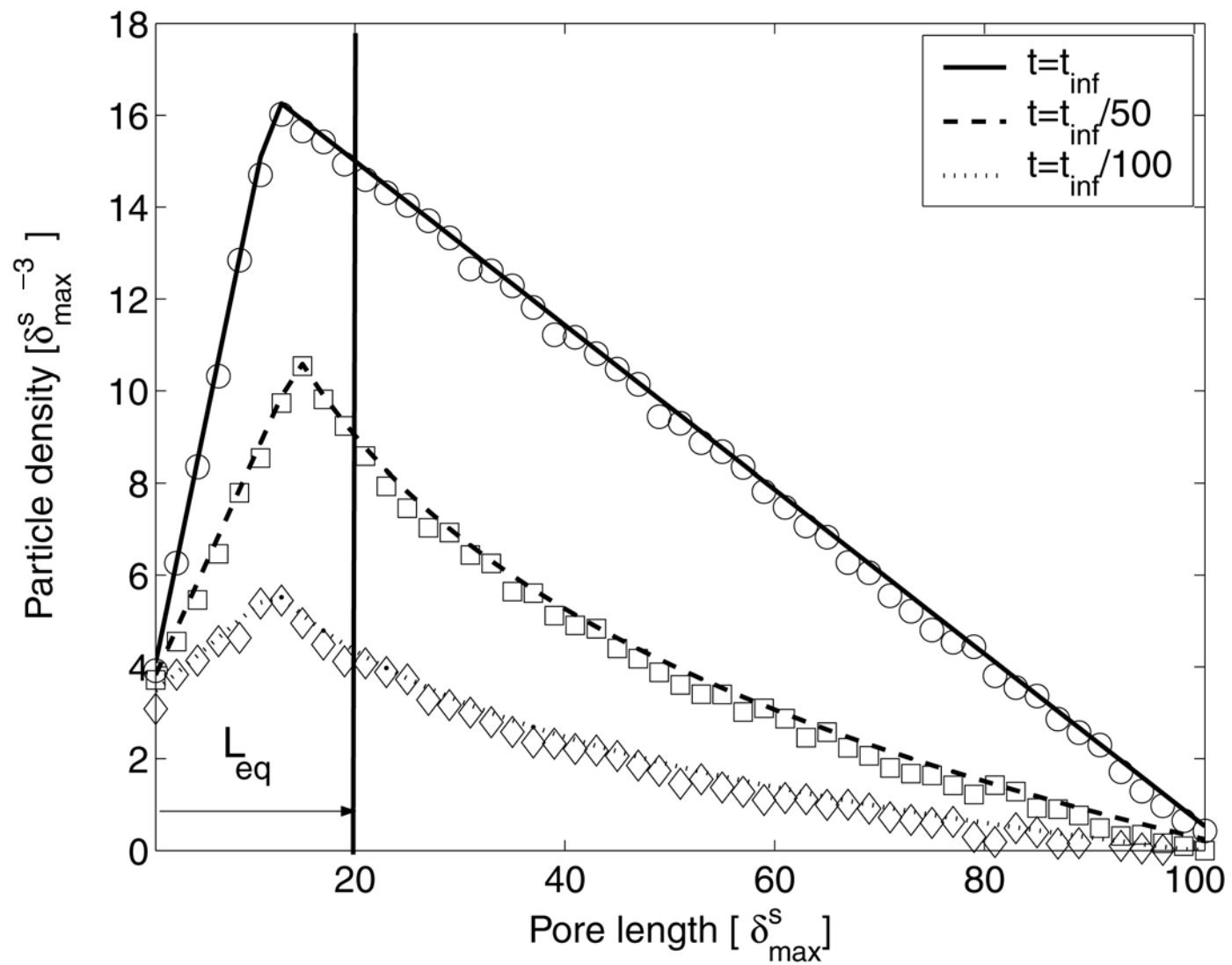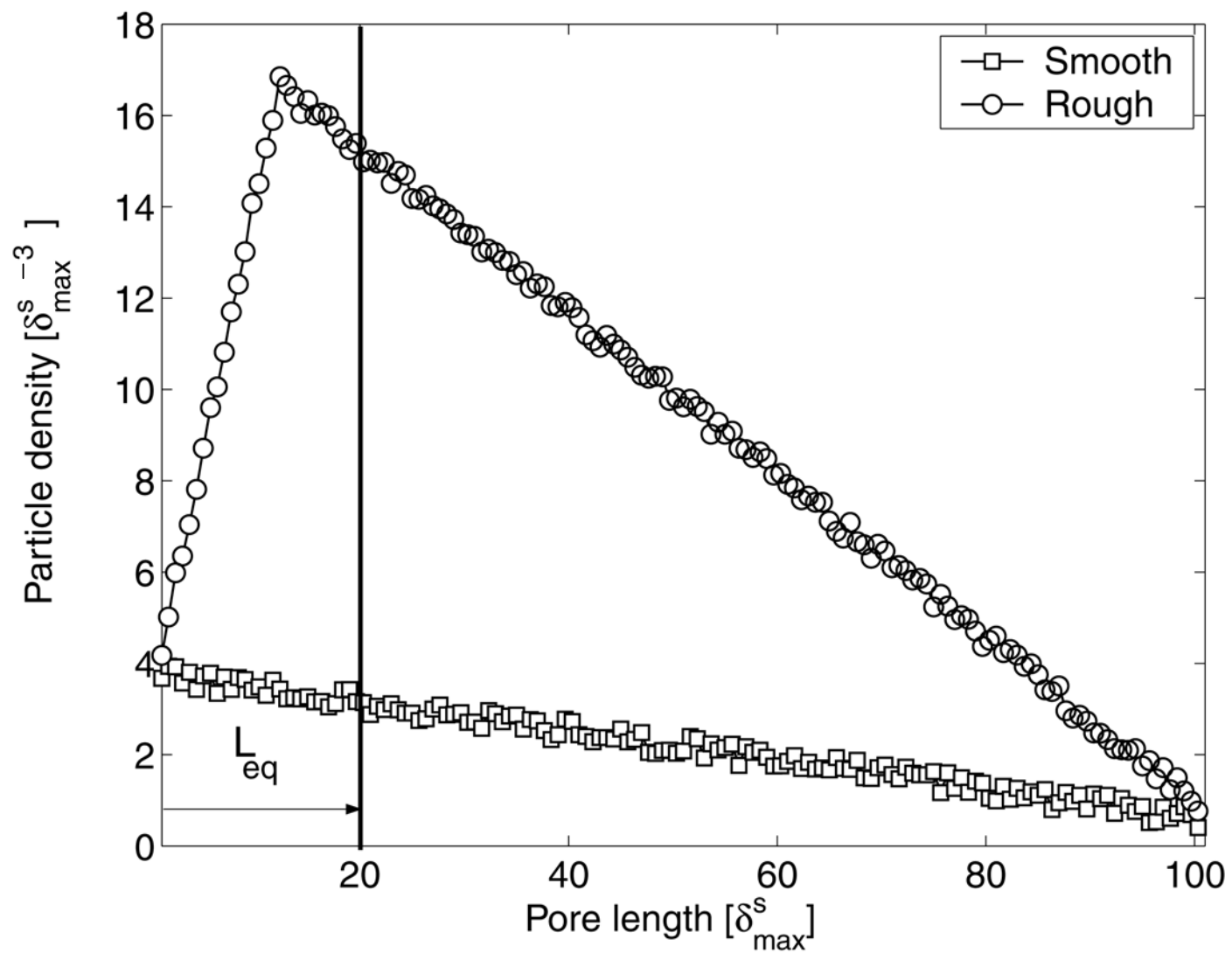Figure 8

| Pore cross section | Pore | Diffusivity |
|---|---|---|
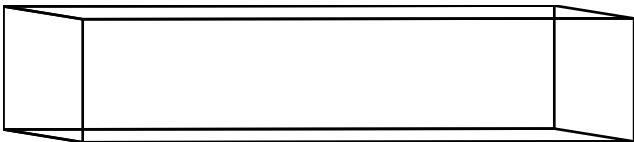
n=0
$D_t$=0.0142
$D_s$=0.0141
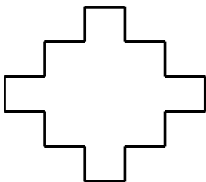
n=1
$D_t$=0.0143
$D_s$=0.0142
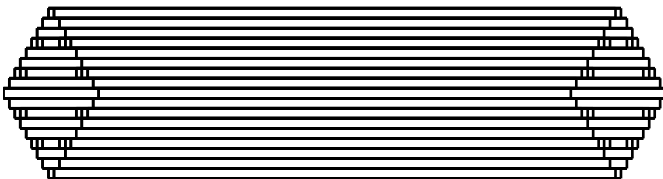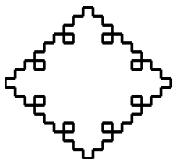
n=2
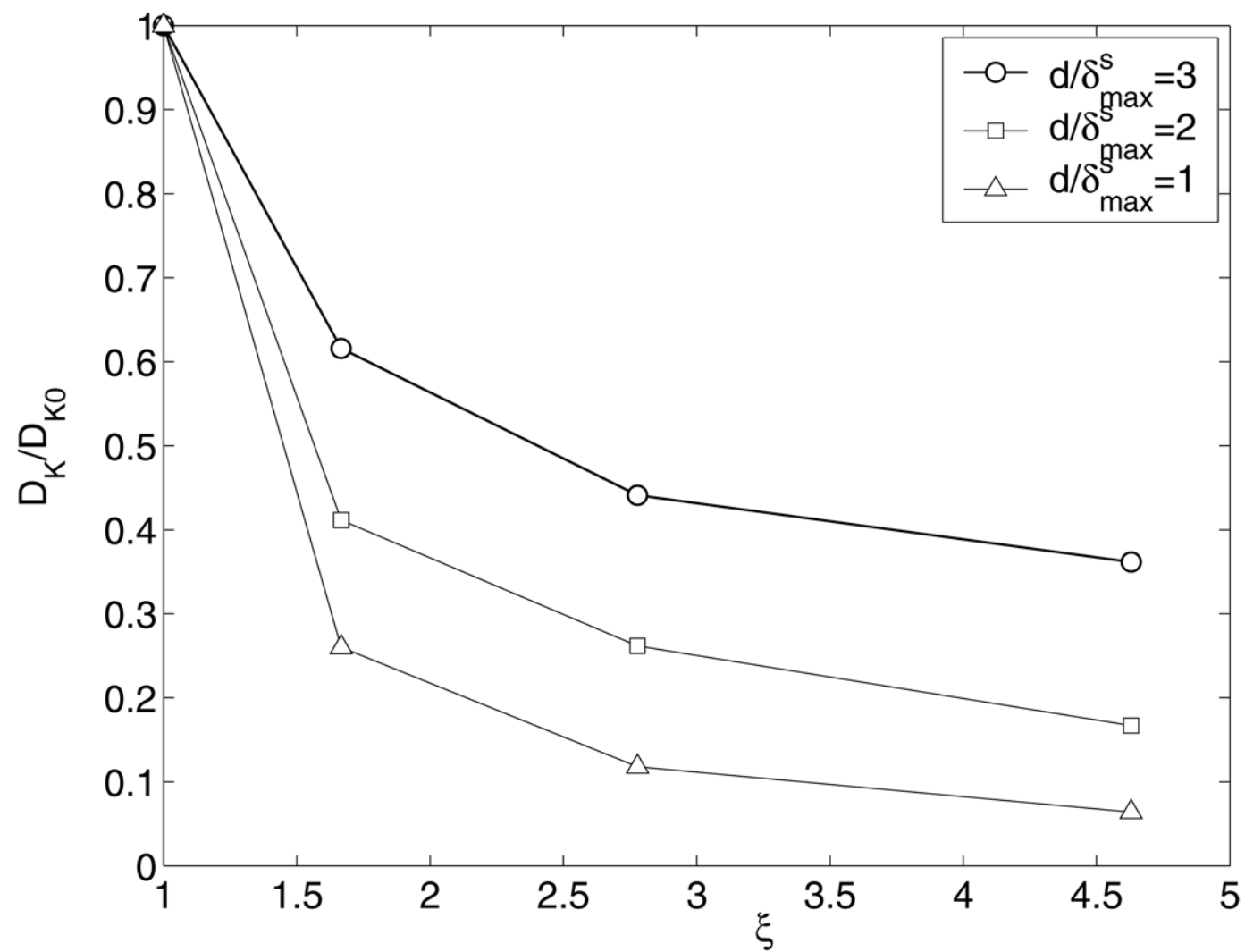$D_t$=0.0142
$D_s$=0.0143
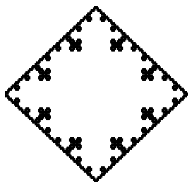
n=3
$D_t$=0.0141
$D_s$=0.0142
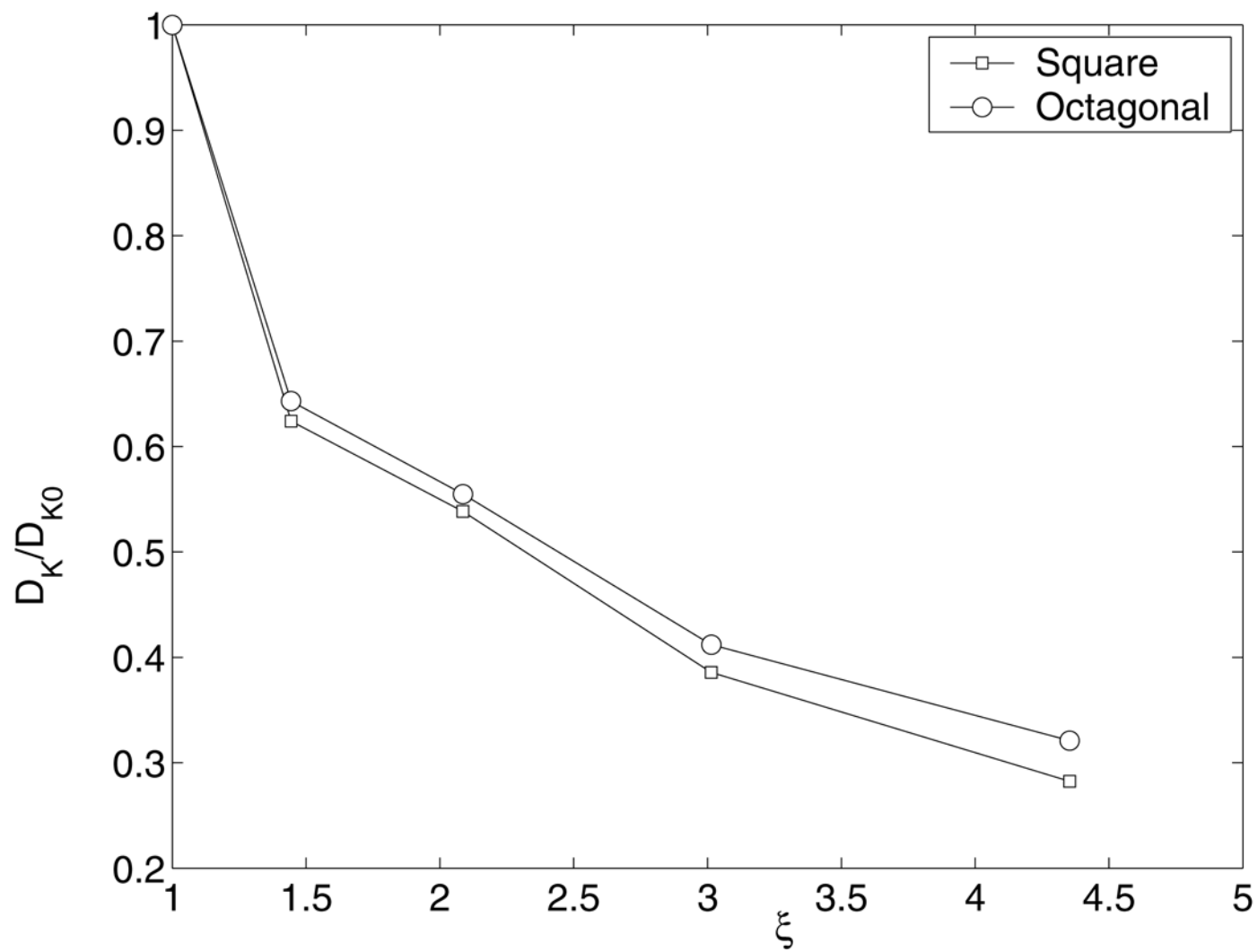
Figure 9a

Figure 9b

Figure 10a

Figure 10b

Figure 11a

Figure 11b